Article

Silicon as a permanent-carbon sedimentation tracer

E. Sikar[1*], B. Matvienko[1], M. A. Santos[2], S. R. Patchineelam[3], E. O. Santos[2**], M. B. Silva[1***], C. H. E. D. Rocha[2****], A. C. P. Cimbleris[4] and L. P. Rosa[2]

[1] *Construmaq São Carlos. Rua Sebastião de Moraes 610. CP 717. São Carlos, SP. 13562-030, Brazil*
[2] *Energy Planning Program/COPPE/UFRJ, Centro de Tecnologia, Bloco C, Sala 211, Cidade Universitária, Rio de Janeiro, RJ. 21941-972, Brazil*
[3] *Departamento de Geoquímica - Universidade Federal Fluminense, Rua Miguel de Frias, 9, 3º andar, Icaraí., Niterói, RJ, 24220-900, Brazil*
[4] *Furnas Centrais Elétricas S.A. Rua Real Grandeza 219, Rio de Janeiro, RJ, 22281-900, Brazil*
[*] *Corresponding author email: elizabeth@linkway.com.br*
[**] *Current address: Departament of Environment Sciences - Federal Rural University of Rio de Janeiro, Rodovia BR 465, km 07, Seropédica, RJ, 23890-000, Brazil*
[***] *Current address: University of Brasília, Área Especial 02 Lote 14 Setor Central, Gama, DF. 72405-610, Brazil*
[****] *Current address: IBRAM. SEPN 511 - Bloco C - Edifício Bittar, Brasília, DF, 70750-543, Brazil*

Received 30 October 2011; accepted 16 May 2012; published 26 June 2012

Abstract

A procedure to quantify permanent carbon (C) sedimentation rates was required to compare these rates to methane (CH_4) and carbon dioxide (CO_2) water–air emission rates measured during reservoir C flux studies. Therefore, a new method to estimate C burial rates using silicon (Si) as a tracer was devised and applied. Burial rates in 8 tropical reservoirs were measured. Ages of these 8 reservoirs varied between 3.7 and 49 years. Each reservoir was surveyed 3 times during 1 year. Median burial rate was 78 (min 12, max 516; n = 66) mg C m^{-2} d^{-1}. Trapped C (C_t) rates were also measured; the resulting median was 845 mg C m^{-2} d^{-1} (min 179, max 19 064; n = 40). Burial efficiency (comparison between C burial rate and C_t rate) was ~10%. Carbon burial efficiency of the 8 reservoirs showed strong dependence on bottom water temperature, efficiency being halved for each 3.4 °C increase in annual average temperature of reservoir bottom water. This finding strongly supported the adequacy of the Si-tracer method for rate measurements of carbon burial in sediments. Simultaneous with our new Si-tracer method we conducted traditional lead 210 isotope (^{210}Pb) dating. The resulting median was 133 (min 11, max 441; n = 15) mg C m^{-2} d^{-1}. Compared to the Si-tracer median, the ^{210}Pb-dating technique resulted in a higher C median burial rate because the sampling sites that lacked sediment (and therefore contributed a null burial rate) were, in retrospect, erroneously disregarded.

Key words: carbon burial efficiency, carbon daily burial rates, sediments, silicon as sedimentation tracer, temperature sensitivity, tropical hydroelectric reservoirs

Introduction

Tropical lakes and reservoirs are complex and dynamic environments (Tundisi 1999, Tranvik et al. 2009) presenting variability in space (Santos et al. 2005, Assireu et al. 2007) and over a time scale as short as one day (Lima et al. 2005). They can both emit carbon (C) into the atmosphere and absorb it through the water–air interface depending on limnologic and hydrologic conditions (Abril et al. 2005). At the same time, as organic debris sinks in the water column, passing through trophogenic and tropholytic zones (Bloesch 2004), reactivity of organic matter decreases (Middelburg 1989), and eventually organic C fossilizes in the sediments.

Organic C daily depositional rates, here also called trapped C (C_t), in reservoirs are directly measurable with

DOI: 10.5268/IW-2.3.465

sample-collecting sedimentation traps and gravimetric procedures to quantify these samples. In contrast, C daily burial rates are not directly measurable because the fraction of the C daily deposition that will undergo further decomposition—and eventually return to the water column as dissolved organic C, methane (CH_4), and carbon dioxide (CO_2)—is unknown. Therefore, in the absence of sediment resuspension, C_t rates in younger reservoirs are higher than C daily burial rates.

Our measurements of tropical reservoir C fluxes were designed to establish individual C budgets for each of the 8 studied reservoirs. In addition to measuring C daily fluxes between air and water, we needed measurements of permanent C sedimentation using a method sensitive enough to detect daily variations. The time resolution provided by the lead 210 isotope (^{210}Pb) dating method was too coarse for our study of C daily fluxes in reservoirs. A tracer to refine the estimates of C daily burial rates was needed.

Silicon (Si) is present in the Earth's crust in many forms such as silica (SiO_2) and clay and is also found in water bodies (Goto et al. 2007) as well as in lacustrine and estuarine sediments (Vaalgamaa and Korhola 2007). Although its origin can be either minerogenic or biogenic (e.g., diatoms), it is mostly minerogenic in the set of tropical reservoirs in this study (VLM Huszar, National Museum of the Federal University of Rio de Janeiro, and F Roland, Federal University of Juiz de Fora, November 2007, pers. comm.). Clay-bearing muddy waters of inflowing rivers were often seen by the authors; furthermore, infrared spectroscopy and x-ray diffraction characterization of trapped particles in the low Amazon region showed presence of aluminosilicates that also are of mineral origin (Moreira-Turcq et al. 2004).

Si and C inflows reflect changes in land use (e.g., agriculture and cattle-grazing; Santos et al. 2009). Within water bodies, SiO_2 and clay together with organic detritus eventually sink to bottom. Because these and the lower reaches of tropical reservoirs are anoxic due to intense biological activity and water stratification, they usually present environments with pH <6. The acidic condition renders the Si-containing substances insoluble; thus, their Si content becomes suitable for use as a permanent C sedimentation tracer. Unlike Si, iron (Fe), which is also abundant in the sedimentation traps, cannot be used as a tracer because inside the acidic and anoxic sediment the insoluble Fe^3 is reduced to the relatively soluble Fe^2, which then diffuses back into the water (Brayner and Matvienko 2003).

Finally, the research question in this study is: having measured a reservoir's C emission rate (in mg m^{-2} d^{-1}) into the atmosphere, what is the C sequestration rate (in mg m^{-2} d^{-1}) into the permanent sediment layer?

Study sites

Eight representative reservoirs (Fig. 1) were chosen for C budget studies from a larger set of Furnas reservoirs to span a wide range of latitudes and reservoir ages. The surveyed reservoir areas comprise 4096 km^2. Geographical coordinates of the C burial measurement sites (Table 1) were chosen based on a compromise between representativeness and logistic constraints (see details in Supporting Information [SI]).

Methods

Over a 5-year period (2003–2007), 27 field campaigns of up to 2 weeks were carried out in Brazil as part of a study called the "Carbon Budget Project in Furnas Reservoirs" (see SI for further details).

Carbon burial quantified with three measurements: Three measurements were needed to obtain the permanent C sedimentation rate, expressed as mg C m^{-2} d^{-1} using Si as a tracer: Si settling rate in mg Si m^{-2} d^{-1}; Si concentration [Si] profile of the sediment (% Si); and the C concentration [C] profile of the sediment (% C).

Once the sedimentation rate (T) of Si was determined through the use of sediment traps and the C to Si ratio (Q; %C/%Si) within the permanent sediment layer was established, then the permanent C sedimentation rate (P) was determined by $P = T \times Q$. The permanent C sedimentation (or C burial) rate P was expressed in mg C m^{-2} d^{-1}. In other words, carbon daily burial rates were not measured directly; rather, they were inferred by multiplying the C/Si ratio by the Si daily settling rates.

Carbon daily burial rates in this study (Table 1), estimated using the ^{210}Pb dating method, were obtained by dividing the measured rate (given in g C m^{-2} yr^{-1}) by 365 (resulting g C m^{-2} d^{-1}). Although for our purposes the ^{210}Pb-dating technique was not adequate, we used it to ensure that the range of C burial results obtained with the new Si-tracer method was within the range yielded by the well-established ^{210}Pb method; C burial rates were independently obtained from both methods. The ^{210}Pb method rates were used as a reference of comparison for our Si tracer. Another measurement performed, although not strictly necessary, was C_t (see SI for further discussion).

Silicon settling rate: Our sedimentation traps were made of polyvinyl chloride (PVC) tubes 40 cm in length (h), 7.1 cm diameter (dia), and closed at the bottom. To minimize trap interference in the measurements, aspect ratio (h/dia) 5.6 was used (Rosa et al. 1994; see SI for traps details).

In the laboratory, the water from the trap was filtered (0.45 µm pore size paper filter); more than one filter was used when filtering speed became too low due to filter

 DOI: 10.5268/IW-2.3.465

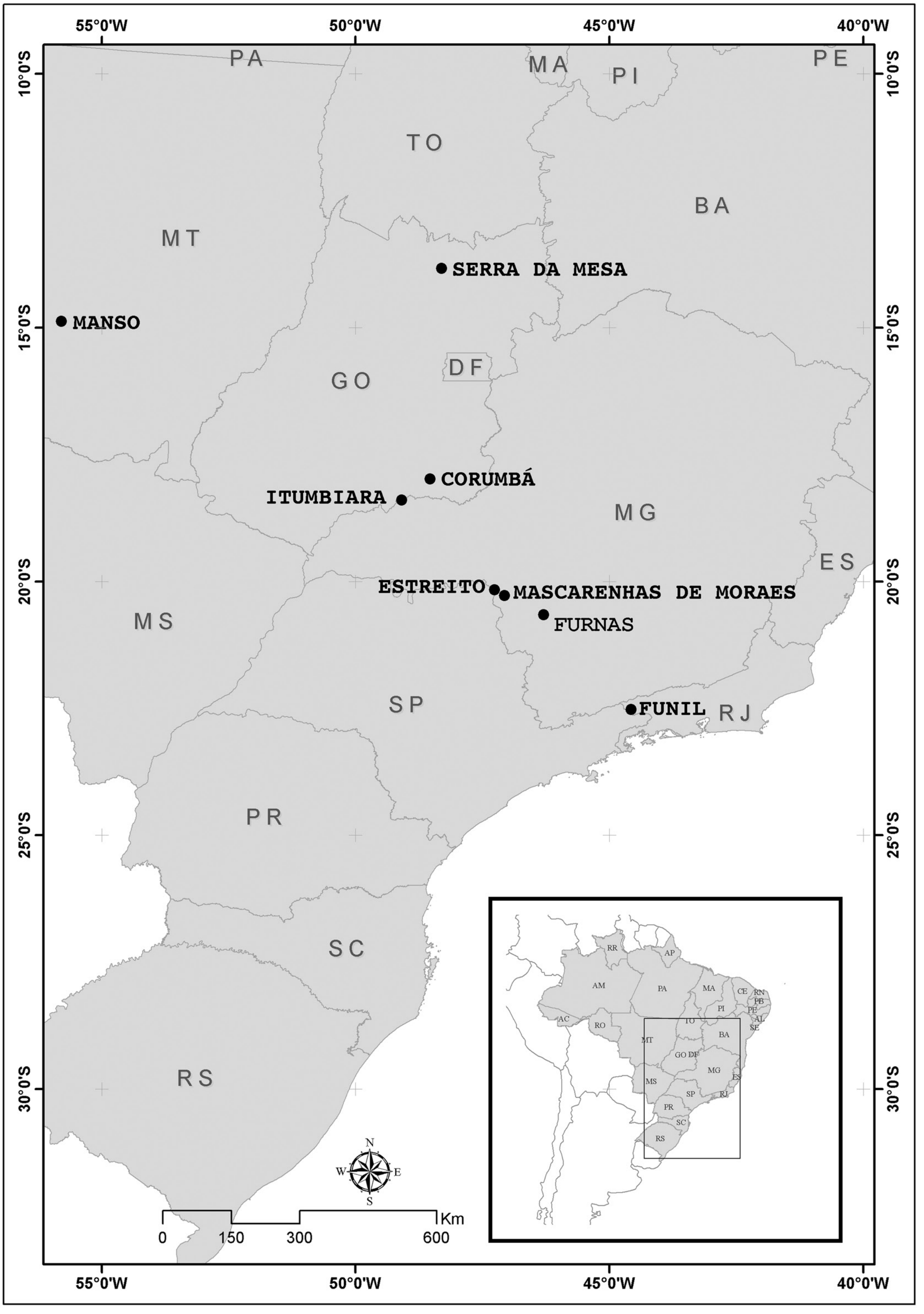

Fig. 1. Location of the 8 sampled Brazilian reservoirs.

Table 1. Geographical coordinates (DEG/MIN/SEC) of sediment coring sites; C and Si median concentrations (in brackets) in sediment cores; geographical coordinates of traps used to measure settling rates of Si. Adjacent to these traps, starting from the Corumbá/2(03/05) survey onward, traps were also installed to measure trapped carbon (C_t) rates; Si settling rates measured with traps; carbon burial rates measured using silicon as a tracer (C(Si)); carbon burial rates measured with ^{210}Pb dating (C(^{210}Pb)) ±standard deviation (SD); (C_t) measured with traps.

Reservoir/ campaign (month/year)	Sediment core site		[C] in core slices, (%C) (min;max;n)	[Si] in core slices ;(%Si) (min;max;n)	Trap site		Si settling rate (mg Si m^{-2} d^{-1})	C(Si) (mg C m^{-2} d^{-1})	C (^{210}Pb) (mg C m^{-2} d^{-1})±SD	Ct (mg C m^{-2} d^{-1})
	Latitude (S)	Longitude (W)			Latitude (S)	Longitude (W)				
Serra da Mesa/1(11/03)	13°48’46”	48°20’02”	3.23 (1.89;4.28;3)	34.4 (16.0;34.6;3)	13°48’46”	48°20’02”	596	56	—	—
	13°48’46”	48°20’02”	4.58 (3.66;5.51;2)	35.4 (34.9;35.9;2)				77	—	—
	13°49’26”	48°18’48”	1.36 (1.30;1.95;3)	33.1 (9.93;34.1;3)	13°49’26”	48°18’48”	475	20	—	—
	13°49’26”	48°18’48”	1.25 (1.21;1.52;3)	32.0 (29.5;37.3;3)				19	—	—
	14°31’04”	49°18’48”	2.29 (1.41;3.09;3)	33.2 (31.8;34.6;2)	14°31’04”	49°02’28”	351	24	—	—
	14°19’44”	49°00’22”	3.50 (3.24;5.26;3)	17.1 (10.5;34.1;3)	14°31’04”	49°02’28”	459	94	—	—
Serra da Mesa/2(03/04)	13°48’46”	48°20’02”	3.33 (2.18;4.47;2)	19.4 (18.2;20.5;2)	13°48’45.4”	48°20’1.5”	770	132	—	—
					13°48’45.4”	48°20’1.5”	460	79	—	—
					13°48’45.4”	48°20’1.5”	410	70	—	—
					13°48’45.4”	48°20’1.5”	620	106	—	—
	14°31’04”	49°18’48”	2.98 (2.83;3.63;2)	26.7 (8.70;33.9;3)	14°31’05.8”	49°02’25.2”	2060	230	—	—
	14°31’04”	49°18’48”	3.15 (3.12;3.81;3)	17.6 (12.8;18.0;3)	14°31’05.8”	49°02’25.2”	2880	515	—	—
	14°31’04”	49°18’48”	4.29 (n=1)	15.8 (n=1)	14°31’05.8”	49°02’25.2”	1900	516	—	—
	14°31’04”	49°18’48”	4.79 (3.34;6.23;2)	20.4 (16.7;24.0;2)	14°31’05.8”	49°02’25.2”	1480	348	—	—
Serra da Mesa/3(07/04)	13°48’29.6”	48°19’54.4”	1.31 (n=1)	21.0 (n=1)	—	—	—	—	—	—
	13°48’29.6”	48°19’54.4”	5.32 (2.94;5.96;3)	7.71 (0.03;20.7;3)	—	—	—	—	—	—
	—	—	—	—	14°02’29.5”	48°26’57.8”	460	—	—	—
	—	—	—	—	14°25’53.8”	48°58’55.2”	716	—	—	—

— not measured or unavailable data

DOI: 10.5268/IW-2.3.465

Table 1. *Continued*

Reservoir/ campaign (month/year)	Sediment core site		[C] in core slices, (%C) (min;max;n)	[Si] in core slices ;(%Si) (min;max;n)	Trap site		Si settling rate (mg Si m^{-2} d^{-1})	C(Si) (mg C m^{-2} d^{-1})	C (^{210}Pb) (mg C m^{-2} d^{-1})±SD	Ct (mg C m^{-2} d^{-1})
	Latitude (S)	Longitude (W)			Latitude (S)	Longitude (W)				
Manso/1(11/03)	14°53'16"	55°47'11"	3.64 (3.27;5.73;5)	31.0 (27.3;37.3;4)	14°54'33"	55°45'52"	1110	130	—	—
Manso/2(03/04)	14°53'16"	55°47'11"	0.42 (0.36;0.50;7)	16.8 (10.4;25.5;7)	14°53'19.3"	55°47'10.1"	2280	57	—	—
					15°00'05.1"	55°39'23.8"	1860	47		
Manso/3(07/04)	15°03'36.1"	55°43'31.5"	1.37 (n=1)	26.4 (n=1)	14°49'13.4"	55°37'58.9"	1253	65	—	—
	15°04'26.1"	55°42'00.3"	1.38 (1.14;1.60;3)	31.0 (27.2;35,0;3)	15°00'23.9"	55°39'00.6"	1390	62		
Corumbá/ 1(11/04)	17°47'12.3"	48°35'40.5"	1.16 (0.42;2.50;6)	20.6 (18.0;23.2;2)	17°47'16.4"	48°35'29.3"	210	12	114±6	—
	17°45'28.8"	48°33'51.5"	2.27 (0.72;3.07;6)	9.86 (4.81;21.5;6)				48	134±7	
Corumbá/ 2(03/05)	17°46'9.7"	48°34'7.9"	2.15 (2.03;2.81;3)	13.4 (8.19;26.2;3)	17°45'57.9"	48°34'08.7"	311	50	—	3810
					17°45'57.9"	48°34'08.7"	440	71		3200
Corumbá/ 3(08/05)	17°46'09"	48°34'07"	1.90 (1.49;2.40;9)	4.52 (2.22;6.54;4)	17°46'10.1"	48°33'20.5"	340	143	133±7	1270
Itumbiara/ 1(11/04)	18°18'52.5"	48°02'5.1"	2.43 (1.59;3.24;6)	6.14 (3.01;9.55;5)	18°18'45.4"	49°0.2'02.4"	88	35	136±7	—
Itumbiara/ 2(03/05)	18°18'39"	48°35'12.2"	2.91 (2.57;3.24;2)	11.7 (8.61; 14.9; 2)	18°21'59.4"	48°38'24.0"	171	43	—	1350*
					18°21'59.4"	48°38'24.0"	390	97		
					18°20'31.1"	48°38'18.6"	228	57		
	18°16'59.1"	48°54'20"	2.48 (2.13;2.83;2)	5.86 (5.76 ; 5.96 ; 2)	18°17'0.6"	48°54'21.3"	109	46		864
					18°17'0.6"	48°54'21.3"	116	49		
					18°17'0.6"	48°54'21.3"	96	41		
Itumbiara/ 3(08/05)	18°15'14.9"	48°55'25.2"	2.72 (2.14;3.16;15)	9.15 (5.05 ; 13.1 ; 10)	18°22'19"	48°43'28"	152	45	242±12	583
	18°22'39.2"	48°47'52.1"	1.73 (0.41;2.99;11)	8.56 (7.04 ; 12.2;4)	18°22'19"	48°43'28"	255	52	70±4	552
					18°23'11"	48°43'58"	115	23		386
Estreito/1(11/05)	20°09'42.6"	47°17'8.8"	3.08 (2.49;3.43;5)	11.7 (9.3;19.7;5)	—	—	—	—	—	—
Estreito/2(03/06)	20°09'42.6"	47°17'8.8"	2.47 (1.83;5.10;8)	28.2 (21.7;32.2;3)	20°10'05.7"	47°16'11.7"	2169	190	—	2697
					20°10'05.7"	47°16'11.7"	2291	200		19064
Estreito/3(08/06)	20°10'4.4"	47°16'12.3"	2.52 (2.26;2.90;7)	7.73 (6.38;8.63;4)	20°10'03.8"	47°16'08.7"	292	95	—	415
					20°10'05.7"	47°16'11.7"	338	110		531

— not measured or unavailable data ; * trap installed midway between 18°21'59.4"S 48°38'24.0"W and 18°20'31.1"S 48°38'18.6"W

Table 1. *Continued*

Reservoir/ campaign (month/year)	Sediment core site Latitude (S)	Sediment core site Longitude (W)	[C] in core slices, (%C) (min;max;n)	[Si] in core slices ;(%Si) (min;max;n)	Trap site Latitude (S)	Trap site Longitude (W)	Si settling rate (mg Si m^{-2} d^{-1})	C(Si) (mg C m^{-2} d^{-1})	C (^{210}Pb) (mg C m^{-2} d^{-1})±SD	Ct (mg C m^{-2} d^{-1})
Mascarenhas de Moraes/1(11/05)	20°25’0.8”	46°58’11.6”	2.95 (2.73;3.73;20)	6.08 (4.29;6.94;6)	20°23’25.6”	46°57’33.7”	196	95	441±22	806
					20°23’25.6”	46°57’33.7”	182	88		
Mascarenhas de Moraes/2(04/06)	20°24’57.9”	46°58’15.2”	3.37 (3.09;4.02;20)	15.2 (7.73;16.6;5)	20°23’21.1”	46°57’28.7”	473	105	42±4	564
					20°23’21.1”	46°57’28.7”	1173	260		
Mascarenhas de Moraes/3(08/06)	20°24’57.9”	46°58’15.2”	2.41 (2.07;2.57;16)	8.38 (4.38;11.1;7)	20°23’22.3”	46°57’41.6”	93	27	11±1	223
					20°23’12.6”	46°57’43.1”	195	56		316
Furnas/1(11/05)	21°05’18.1”	46°05’33.1”	4.70 (3.68;14.9;6)	5.31 (3.71;6.21;6)	21°02’13.2”	46°02’46.5”	352	312	—	1381
					21°02’13.2”	46°02’46.5”	207	183		378
	20°45’29.4”	45°55’27.7”	2.13 (0.53;3.30;13)	8.89 (4.91;13.4;6)	20°44’44.0”	45°55’43.3”	158	38	169±9	822
					20°44’44.0”	45°55’43.3”	396	95		460
Furnas/2(04/06)	20°45’29.4”	45°55’27.7”	2.92 (1.41;3.88;15)	12.0 (6.47;13.1;8)	21°01’45.3”	46°05’25.7”	1009	246	73±4	1516
					21°01’40.8”	46°05’26.3”	1383	337		1183
					20°44’54.8”	45°55’44.9”	431	105		589
					20°44’52.2”	45°55’44.0”	278	68		1129
Furnas/3(08/06)	20°45’29.4”	45°55’27.7”	1.44 (0.99;2.75;18)	6.40 (4.71;10.1;8)	20°57’15.5”	46°03’51.4”	219	49	135±13	542
					20°57’15.5”	46°03’51.4”	143	32		807
					20°44’59.8”	45°55’44.3”	138	31		179
					20°44’59.8”	45°55’44.3”	187	42		302
Funil/1(11/06)	22°31’33.3”	44°32’55.9”	1.56 (1.28;2.31;18)	0.88 (0.35;1.45;8)	22°31’43.9”	44°33’24.2”	87	154	—	3200
					22°31’43.9”	44°33’24.2”	121	215		6342
Funil/2(03/07)	22°31’33.3”	44°32’55.9”	1.37 (1.02;2.12;15)	1.62 (0.82;3.06;9)	22°31’42.1”	44°33’19.4”	330	279	38±2	2016
					22°31’42.5”	44°33’19.4”	95	80		1999
Funil/3(07/07)	22°31’33.3”	44°32’55.9”	2.19 (1.66;3.17;16)	2.25 (0.41;2.45;7)	22°31’44.9”	44°33’23.2”	384	374	355±36	984
					22°31’42.6”	44°33’19.3”	94	91		1184
Manso/4(11/06)	14°53’15.8”	55°47’11.1”	1.36 (0.79;2.64;10)	4.44 (1.61;6.09;5)	14°50’36.1”	55°42’55.4”	60	18	38±2	368
					14°50’43.4”	55°42’51.6”	139	43		826
Manso/5(03/07)	14°53’15.6”	55°47’11.5”	1.80 (0.85;2.89;5)	3.85 (2.05;4.90;3)	14°50’34.6”	55°42’28.0”	454	212	—	2878
					14°50’43.6”	55°42’49.8”	407	190		1841
Manso/6(07/07)	—	—	—	—	14°50’39.5”	55°42’45.9”	251	—	—	885
					14°50’45.7”	55°42’45.6”	117			600

— not measured or unavailable data

DOI: 10.5268/IW-2.3.465

clogging (Fig. S-2 in SI). The filters retained all the particulate Si that passed through the trap's mouth (see Fig. S-3 in SI for 4 representative filtrates).

Filter papers with the filtered solids were then subjected to alkaline fusion (Jackson 1958) to bring Si into solution as sodium silicate. Folded filter papers (still wet, or dried at room temperature) were cut to fit in a 65 mL nickel crucible; 20 mL of 1 M NaOH were added and the mixture was digested and dried for 30 min on a 600 Watt, 12 cm dia hot plate. The crucible was then heated in a furnace, reaching 800–900 °C in 40–60 min. An additional 10–15 min was allowed to conclude fusion. The methods for the dissolution and analysis of the alkaline melt produce a silicate solution similar to solution S, which is obtained from the alkaline fusion of sediment samples (solution S and procedure described below in Alkaline fusion and analysis of sediment silica; see SI for methods to obtain C_t filtrate).

Sediment coring: Cores were taken from the reservoir bottom using a Niederreiter corer (made by UWITEC), a tube corer equipped with a lower-end closure device. We rejected cores that included roots and twigs because this material introduces outliers into the set of measured C concentrations.

The cores were cut into horizontal slices 1–3 cm thick, depending on sediment consistency, and stored in plastic bags until reaching the laboratory where C and Si concentrations in the slices were determined.

Organic carbon: Organic C in the sediment was determined using an SSM-5000A Shimadzu C analyzer (see SI for measurement of organic C concentration in the C_t).

Alkaline fusion and analysis of sediment silica: We followed a modified method described in Jackson (1958) and Mackereth et al. (1978) for alkaline fusion and analysis of sediment silica. From the sediment sample (previously dried at 110 °C for 1 h and crushed), a 50 mg aliquot was precisely weighed in a 35 mL platinum (Pt) crucible and mixed with Na_2CO_3 four times its mass. The Pt crucible was then placed on an alumina-sheathed triangle on a tripod and heated with a torch to bright red (800–900 °C), which required <1 min. After cooling, 100 mL of distilled water was used to dissolve the alkaline melt and to rinse the crucible. Solution and rinsing water were combined in a polyethylene beaker (as opposed to a glass beaker to avoid possible addition of Si) and then filtered through a paper filter, neutralized with 1 M HCl to pH 7, and completed with distilled water to 150 mL. The resulting silicate solution was called solution S.

Next, Si content was determined by the silico-molybdic yellow method; 20 mL of solution S were transferred to a polyethylene beaker, to which 2 mL of freshly prepared 0.1 M ammonium molybdate solution was added and stirred. After a 15 min rest, 5 mL of 1:1 H_2SO_4 solution was added, followed by a 10–15 min rest.

Absorbance A (the base 10 logarithm of the blank-to-sample transmittance ratio, which in spectrophotometric analysis is the commonly used definition for absorbance) was then determined against a blank at wavelength $\lambda = 410$ nm and compared to absorbance of an Si standard solution. For these analytical conditions and for a 1 cm optical path length, the linear relationship between absorbance A and the [Si] in g Si L^{-1} in the analyzed solution S was expressed by

$$[Si] = 0.000534 + 0.1347\ A. \quad (1)$$

Estimated error for absorbance up to A = 0.15 was <5% (measurement of $C(^{210}Pb)$ described in SI).

Strength and statistical significance of correlations between datasets: Strength, polarity, and statistical significance of correlations were analyzed in this work with correlation coefficient (R), R signal (e.g., +R and –R), and the P-value (P), respectively, using the binary criteria (Table 2).

Results and Discussion

Comparison between C(Si) and $C(^{210}Pb)$ medians: Carbon burial rates ranged between 12 and 516 (median 78; n = 66) mg C m^{-2} d^{-1} for C(Si), and between 11 and 441 (median 133 ; n = 15) mg C m^{-2} d^{-1} for $C(^{210}Pb)$. A significant correlation between C burial rate and reservoir age was found only for the older reservoirs (17+ years; see details in SI).

Range of [C] in sediment core slices: The [C] increase rate of 0.018% C cm^{-1} ($P < 0.001$, solid line in Fig. 2) toward the sediment core top is relatively similar to the 0.014% C cm^{-1} rate obtained for sediments sampled in older reservoirs ($P < 0.01$, dashed line in Fig. 2), possibly due to residual decomposition in the sediments (see SI for

Table 2. Criteria used in this work for evaluating the correlation between two datasets.

CORRELATION CHARACTERISTIC	DEFINITION
Positive	R is positive
Negative	R is negative
Strong	$\|R\|^{\dagger} > 0.50$
Weak	$\|R\| < 0.50$
Statistically significant (i.e., unlikely to have occurred by chance)	$P < 0.05$
Not statistically significant	$P > 0.05$

† |R| = absolute value of R

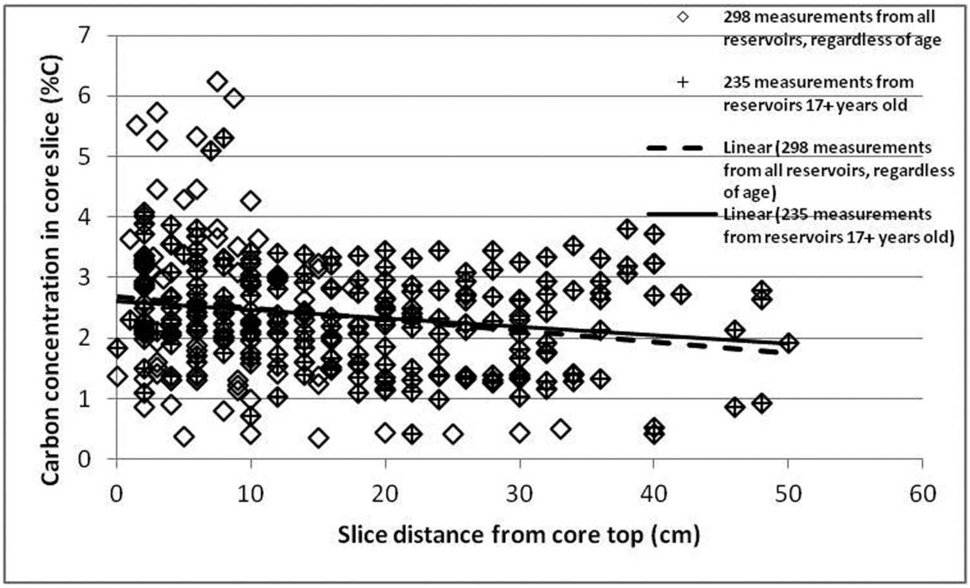

Fig. 2. Carbon concentrations [C] in all 298 core slices sampled during this study. Results of the 2 core slices with highest [C] are not shown: 10.1%C (at depth 10.1 cm) and 14.9%C (12 cm).

further information on range and variety of [C] in core slices).

When the Si-tracer method was first conceived, we imagined that [C] in sediments would be higher at the sediment surface and would gradually decrease with depth to a constant value regardless of further depth increase. Our results indicate that although this is essentially true, the upper layer where the bulk of final stabilization occurs is surprisingly thin, corresponding to much less than a 1-year deposition of sediment. This layer is about 1 mm thick at 5 m water depth (Gentzel et al. 2012), where in previous studies we observed maximum bubble-CH_4 production. In addition, this layer is more like thick slurry and less like firm sediment and would normally be discarded as overlying water (such discarding does not affect either of the 2 methods here used). Also, the [C] profile variety might be elucidated by studies of the biochemistry in the water column (Bada and Lee 1977, Ogura 1977, Smith et al. 1995, Amon and Fitznar 2001) and by the recent finding of generation of microbial methane in an oxygenated water environment (Grossart et al. 2011).

Correlation between burial efficiency and temperature: Burial efficiency is here expressed as the ratio between permanently buried carbon and C_t (more details in SI). Latitudinal variation of the 7 reservoirs in which we measured C_t produced a 4.4 °C variation in reservoir bottom temperature (Table S-1 in SI), at which final stabilization occurs. As bottom temperatures rise, burial efficiency (calculated with C(Si)) drops. More precisely, for each 3.4 °C increase in the bottom temperature of the reservoirs studied, burial efficiency is halved (Fig. 3). The close linear fit ($R = -0.95$, $P < 0.001$, $n = 7$) lends support to this temperature dependence estimate and is consistent with the strongly positive correlation between C mineralization and temperature (Gudasz et al. 2010). In contrast, no correlation was detected between burial efficiencies calculated with C(^{210}Pb) and reservoir bottom temperature (Fig. 3).

A negative correlation between C_t and reservoir age was observed only for older reservoirs. Burial efficiency and reservoir age were positively correlated (more details in SI).

Si settling rates: Si settling rates decreased with reservoir age at a rate of about 12 mg Si m^{-2} yr^{-1} (more in SI).

Si concentration in sediment sample: [Si] in all the sediment core slices that were analyzed ranged from 0.03 to 37.3% (median 8.70, average 12.0, n = 174; more in SI).

Variability within the reservoirs: The existence of significant variability within the limnological environments here studied was confirmed (Table 1; discussion in SI).

Usage of Si from aluminosilicates and quartz: The Si fusion technique used in this study actually measures total Si (aluminosilicates and quartz sand). Although organic matter sorbs on aluminosilicates as opposed to sand, the structure of the filtrate (Fig. S-3 in SI) also shows considerable presence of particulate organic matter (POM), forming an admixture with quartz and aluminosilicates

 DOI: 10.5268/IW-2.3.465

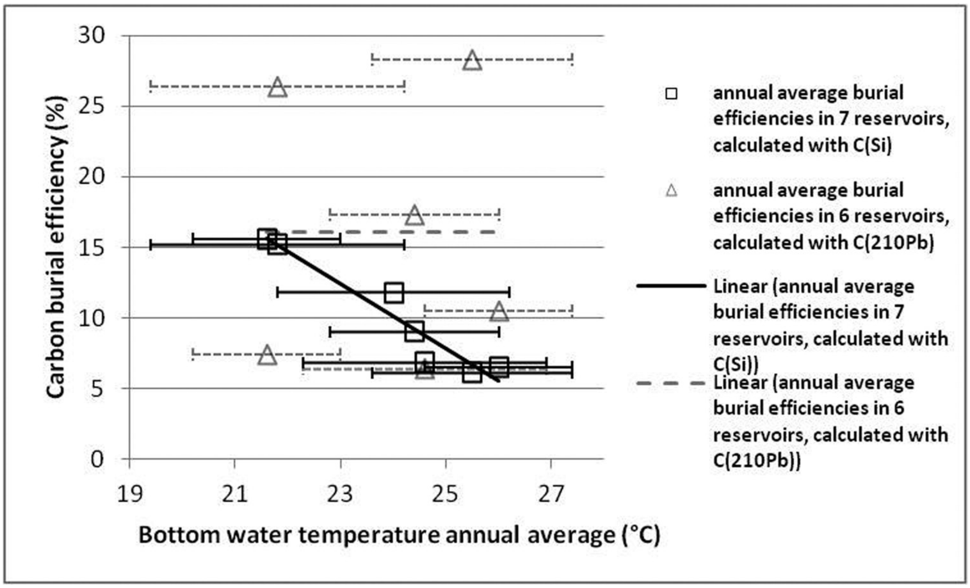

Fig. 3. Burial efficiencies calculated with C(Si) and C(^{210}Pb) were similar (6.9 and 6.4, respectively) for Manso Reservoir (2006–2007 field survey).

alike. Because the Si in sand as well as the Si in aluminosilicates can be tracers of POM, we did not discriminate between Si compounds (SI discusses stability of buried organic matter, resuspension of organic matter and diatom peak abundance).

Conclusions

Carbon daily burial rates here reported were not directly measured but rather were inferred based on the averaged [Si] and [C] profiles in the sediment cores and on the daily settling rates of Si. However, during the analysis of the data, the correlation between C burial efficiency and temperature emerged, supporting these inferred rates. This finding was only possible through the use of the Si method because it is less sensitive than the ^{210}Pb method to sediment dehydration, densification, and spread.

The ^{210}Pb-dating method as applied in this study tended to overestimate burial rates, probably because (1) no register was made of the sediment sampling sites that were disregarded because of sediment dearth, and (2) while this would not affect the C(Si) measurement, it would tend to increase the averages obtained with the ^{210}Pb-dating technique. To avoid this possibility, a null burial rate should have been registered for such sites.

Our study on permanent C settling rates and settling efficiencies in the tropics contributes substantially to the relatively meager datasets available to date. To the best of our knowledge the quantification of temperature-dependence of C burial efficiency, derived from *in situ* measurements at anoxic lake bottoms is the first data of its kind published. With the temperature dependence established for a given reservoir, a simple temperature measurement should allow determination of burial efficiency in situations when the other methods cannot be applied. Multiplying that by the easily measurable C_t rate would be sufficient to calculate permanent C burial rates.

The weak positive correlation between C burial rate and reservoir age, the strong positive correlation between C burial efficiency and reservoir age, and the variety of the [C] profile in sediment cores suggest that organic matter is decomposed mainly in the water column, including the layer of thick slurry above the permanent sediment layer, rather than in the permanent sediment per se, where only residual decomposition takes place.

Acknowledgements

We are grateful to Jürg Bloesch, Sebastian Sobek, Phil Meyers, three anonymous reviewers, editor Christian Kamenik and English text reviser Paula Matvienko-Sikar, for comments that vastly improved this manuscript. We thank Furnas Centrais Elétricas S.A. for research funding and permission to publish.

Supporting Information

Nine figures, one table and more about the study area, method, materials, results and discussion. Available at https://www.fba.org.uk/journals/index.php/IW/issue/view/106.

References

Abril G, Guérin F, Richard S, Delmas R, Galy-Lacaux C, Gosse P, Tremblay A, Varfalvy L, Dos Santos MA, Matvienko B. 2005. Carbon dioxide and methane emissions and the carbon budget of a 10-year old tropical reservoir (Petit Saut, French Guiana). Global Biogeochem Cy. 19:GB4007, doi:10.1029/2005GB002457.

Amon RMW, Fitznar HP. 2001. Linkages among the bioreactivity, chemical composition and diagenetic state of marine dissolved organic matter. Limnol Oceanogr. 46:287–297.

Assireu A, Roland F, Novo E, Barros NO, Stech JL, Pacheco FS. 2007. Existe relação entre a complexidade geométrica do entorno dos reservatórios e a variabilidade espacial dos parâmetros limnológicos? [Is there a relationship between the geometric complexity of reservoir surroundings and spatial variability of limnological parameters?] Portuguese. [cited 28 May 2012]. Available from http://marte.dpi.inpe.br/col/dpi.inpe.br/sbsr%4080/2006/11.14.19.45.28/doc/3263-3269.pdf

Bada JL, Lee C. 1977. Decomposition and alteration of organic compounds dissolved in seawater. Mar Chem. 5:523–534.

Bloesch J. 2004. Sedimentation and lake sediment formation. In: O'Sullivan PE, Reynolds CS, editors. The Lakes Handbook: Limnology and Limnetic Ecology. Oxford (UK): Blackwell Publishing. p. 197–229.

Brayner FMM, Matvienko B. 2003. Manganese and iron as oxygen carriers to anoxic estuarine sediment. J Phys IV France. 107:227–232.

Gentzel T, Hershey AE, Rublee PA, Whalen SC. 2012. Net sediment production of methane, distribution of methanogens and methane-oxidizing bacteria, and utilization of methane-derived carbon in arctic lake. Inland Waters. 2:77–88.

Goto N, Iwata T, Akatsuka T, Ishikawa M, Kihira M, Azumi H, Anbutsu K, Mitamura O. 2007. Environmental factors which influence the sink of silica in the limnetic system of the large monomictic Lake Biwa and its watershed in Japan. Biogeochemistry. 84:285–295.

Grossart HP, Frindte K, Dziallas C, Eckert W, Tang KW. 2011. Microbial methane production in oxygenated water column of an oligotrophic lake. P Natl Acad Sci USA. 108:19657–19661.

Gudasz C, Bastviken D, Steger K, Premke K, Sobek S, Tranvik L. 2010. Temperature-controlled organic carbon mineralization in lake sediments. Nature. 466:478–481.

Jackson ML. 1958. Soil chemical analysis. Englewood Cliffs (NJ): Prentice Hall, Inc.

Lima IBT, Mazzi EA, Carvalho JC, Ometto JPHB, Ramos FM, Stech JL, Novo EMLM. 2005. Photoacoustic/dynamic chamber method for measuring greenhouse gas fluxes in hydroreservoirs. Verh Internat Verein Limnol. 29:603–606.

Mackereth FJH, Heron J, Talling JF. 1978. Water analysis: Some revised methods for limnologists. Freshwater Biological Association; Scientific Publication No. 36.

Moreira-Turcq P, Jouanneau JM, Turcq B, Seyler P, Weber O, Guyot JL. 2004. Carbon sedimentation at Lago Grande de Curuai, a floodplain lake in the low Amazon region: insights into sedimentation rates. Palaeogeogr Palaeoclimatol Palaeoecol. 214:27–40.

Middelburg JJ. 1989. A simple rate model for organic matter decomposition in marine sediments. Geochim Cosmochim Acta. 53:1577–1581.

Ogura N. 1977. High molecular weight organic matter in seawater. Mar Chem. 5:535–549.

Rosa F, Bloesch J, Rathke DE. 1994. Sampling the settling and suspended particulate matter. In: Mudroch A, MacKnight SD, editors. Handbook of techniques for aquatic sediments sampling. Boca Raton (FL): Lewis Publishers. p. 97–129.

Santos EO, Silva C, Santos MA, Matvienko B, Rocha CHEDA, Rosa LP, Sikar E, Silva MB, Bentes AMP Jr. 2009. The importance of land use change analysis in the greenhouse gases emissions from hydroelectric reservoirs. Verh Internat Verein Limnol. 30(6):845–849.

Santos MA, Matvienko B, Rosa LP, Sikar E, Santos EO. 2005. Gross Greenhouse Gas Emissions from Brazilian Hydro Reservoirs. In: Tremblay A, Varfalvy L, Roehm C, Garneau M, editors. Greenhouse gas emissions: fluxes and processes, hydroelectric reservoirs and natural environments. Berlin (Germany): Springer. p. 267–291.

Smith DC, Steward GF, Long RA, Azam F. 1995. Bacterial mediation of carbon fluxes during a diatom bloom in a mesocosm. Deep-Sea Res Pt II. 42:75–97.

Tranvik LJ, Downing JA, Cotner JB, Loiselle SA, Striegl RG, Ballatore TJ, Dillon P, Finlay K, Fortino K, Knoll LB, et al. 2009. Lakes and reservoirs as regulators of carbon cycling and climate. Limnol Oceanogr. 54:2298–2314.

Tundisi JG. 1999. Reservatórios como sistemas complexos: Teoria, aplicações e perspectivas para usos múltiplos. [Reservoirs as complex systems: Theory, applications and prospects for multiple uses.] In: Henry R, editor. Ecologia de reservatórios: estrutura, funções e aspectos sociais. [Reservoir's ecology: structure, functions and social aspects]. Botucatu (Brazil): Fundbio/Fapesp. p.19–38. Portuguese.

Vaalgamaa S, Korhola A. 2007. Geochemical signatures of two different coastal depositional environments within the same catchment. J Paleolimnol. 38:241–260.

DOI: 10.5268/IW-2.3.465